A Large-Scale Quantitative Proteomic Approach To Identifying Sulfur Mustard-Induced Protein Phosphorylation Cascades

ARTICLE *in* CHEMICAL RESEARCH IN TOXICOLOGY · NOVEMBER 2010

Impact Factor: 3.53 · DOI: 10.1021/tx100350x · Source: PubMed

A Large-Scale Quantitative Proteomic Approach To Identifying Sulfur Mustard-Induced Protein Phosphorylation Cascades

Patrick A. Everley* and James F. Dillman III

Research Division, United States Army Medical Research Institute of Chemical Defense, 3100 Ricketts Point Road, Aberdeen Proving Ground, Maryland 21010

Received July 31, 2009

Sulfur mustard [SM, bis-(2-chloroethyl) sulfide] is a potent alkylating agent and chemical weapon. While there are no effective treatments for SM-induced injury, current research focuses on understanding the molecular changes upon SM exposure. Indeed, efforts that seek a more comprehensive analysis of proteins and post-translational modifications are critical for understanding SM-induced toxicity on a more global scale. Furthermore, these studies can uncover proteins previously uncharacterized in SM-exposed cells, which in turn leads to potential targets for therapeutic intervention. Here, we apply a quantitative proteomic approach termed stable isotope-labeling with amino acids in cell culture combined with immobilized metal affinity chromatography to study the large-scale protein phosphorylation changes resulting from SM exposure in a human keratinocyte cell culture model. This resulted in the characterization of over 2300 nonredundant phosphorylation sites, many of which exhibit altered levels in response to SM. Our results point toward several proteins previously implicated in SM-induced toxicity as well as many additional proteins previously uncharacterized. Further de novo analysis of these phosphoproteins using interaction mapping software revealed both known and novel pathways that may serve as future therapeutic targets of SM exposure.

Introduction

The use of sulfur mustard [SM, bis-(2-chloroethyl) sulfide] as a chemical warfare agent dates back to World War I. Unfortunately, there is no current treatment, and relatively little is known about which proteins play a major role in SM-induced toxicity. Indeed, a milieu of signaling molecules respond to SM, triggering many pathways including apoptosis, inflammation, and DNA damage (*1*). Recent reports have shown that SM exposure activates specific proteins, such as p53, NF-κB, Bcl-2, and others (*1*). While these studies are effective at probing individual pathways, they do not put into context the global changes that are occurring in response to SM and how these many signaling pathways intersect; thus, they provide only a limited snapshot of SM-induced toxicity.

Over the past few years, innovations in systems biology and biotechnology have led to important advances in our understanding of biological phenomena. This is due in part to better instrumentation and software development. In particular, the field of proteomics has been accelerated by more accurate and high-throughput mass spectrometry instrumentation. Protein samples that once took hours to evaluate can now be analyzed in a matter of seconds.

Technologies that allow for rapid, sensitive, and specific analysis of the cellular proteome have already proven effective at answering a range of biological questions, from targeted studies to global analyses. For example, metabolic labeling approaches such as stable isotope labeling with amino acids in cell culture (SILAC) (*2*) have proven valuable for studying cell culture models of disease and cellular perturbations. SILAC has been used to study tumor metastasis (*3, 4*), focal adhesion-associated proteins, growth factor signaling, and insulin regulation (*5*). More specifically, SILAC has been employed to study post-translational modifications (PTMs), including methylation (*5*) and phosphorylation (*6*).

The SILAC method employs $^{12}C^{14}N$- and $^{13}C^{15}N$-labeled amino acids added directly to the culture medium, resulting in isotopically "light" and "heavy" cell populations, respectively. Protein samples collected from control (light-labeled) and experimental (heavy-labeled) cells can then be mixed in equal ratios, digested with trypsin, and analyzed by high-resolution mass spectrometry. The corresponding light and heavy peptides from the same protein will coelute during chromatography into the mass spectrometer. Because these peptide ions have the same ionization efficiency, relative quantitative information is obtained for each protein by comparing the signal intensities of the light and heavy peptides in the precursor ion scan (MS scan). Sequence information is then gathered via peptide fragmentation in the fragment ion scan (MS/MS scan). Thus, the incorporation of stable isotopes allows for a quantitative comparison between the two samples. Furthermore, SILAC can be coupled to additional PTM enrichment methods to provide a more specialized understanding of PTM-regulated cellular processes.

Among these PTM enrichment methods is immobilized metal affinity chromatography (IMAC) (*7*) for the isolation of phosphorylated peptides. In short, IMAC employs positively charged metal ions that will bind to negatively charged phosphopeptides from a digested lysate. After an incubation period to allow binding, samples are washed to reduce nonspecificity, and then, phosphopeptides are eluted for subsequent analysis. Recently, this approach has been combined with mass spectrometry to provide a relatively quick and effective means of enriching and identifying thousands of phosphopeptides from biological samples (*6*).

To date, neither SILAC nor IMAC has been applied to the study of SM, and the use of other proteomics methods relating

* To whom correspondence should be addressed. Tel: 410-436-6504. Fax: 410-436-8377. E-mail: patrick.everley@us.army.mil.

10.1021/tx900265z

Report Documentation Page

Form Approved
OMB No. 0704-0188

1. REPORT DATE	2. REPORT TYPE	3. DATES COVERED
2009		**00-00-2009 to 00-00-2009**

4. TITLE AND SUBTITLE	5a. CONTRACT NUMBER
A Large-Scale Quantitative Proteomic Approach To Identifying Sulfur Mustard-Induced Protein Phosphorylation Cascades	5b. GRANT NUMBER
	5c. PROGRAM ELEMENT NUMBER
6. AUTHOR(S)	5d. PROJECT NUMBER
	5e. TASK NUMBER
	5f. WORK UNIT NUMBER
7. PERFORMING ORGANIZATION NAME(S) AND ADDRESS(ES) **United States Army Medical Research Institute of Chemical Defense,Research Division,3100 Ricketts Point Road,Aberdeen Proving Ground,MD,21010**	8. PERFORMING ORGANIZATION REPORT NUMBER
9. SPONSORING/MONITORING AGENCY NAME(S) AND ADDRESS(ES)	10. SPONSOR/MONITOR'S ACRONYM(S)
	11. SPONSOR/MONITOR'S REPORT NUMBER(S)

12. DISTRIBUTION/AVAILABILITY STATEMENT
Approved for public release; distribution unlimited

13. SUPPLEMENTARY NOTES

14. ABSTRACT

15. SUBJECT TERMS

16. SECURITY CLASSIFICATION OF:			17. LIMITATION OF ABSTRACT	18. NUMBER OF PAGES	19a. NAME OF RESPONSIBLE PERSON
a. REPORT	b. ABSTRACT	c. THIS PAGE			
unclassified	**unclassified**	**unclassified**	**Same as Report (SAR)**	**6**	

to SM has been limited. In a recent proteomics study (*8*) of cells treated with radiolabeled SM, two-dimensional gel analysis demonstrated that SM forms adducts with cytoskeletal proteins. While this work provided valuable information on specific targets of SM, it offered a relatively small amount of data given all of the downstream signaling that occurs in response to SM exposure. Alternatively, SILAC has the ability to identify and quantify hundreds of proteins in SM-treated cells, leading to unique insight into the biological response to SM-induced toxicity as well as offering a significant increase in the number of potential therapeutic targets.

Because a large amount of cellular signaling activity is mediated by PTMs such as phosphorylation, here, we present a large-scale quantitative analysis of the phosphoproteome using SILAC and IMAC in a human keratinocyte model of SM-induced toxicity [immortalized human keratinocyte line (HaCaT) cells (*9, 10*)]. Furthermore, we show that the levels of numerous protein phosphorylation sites are altered in response to SM and that many of these resulting changes in SM-exposed cells were previously unknown.

Experimental Procedures

Cell Culture, Metabolic Labeling, SM Exposure, and Lysate Preparation. For SILAC labeling, HaCaT cells were cultured in arginine (Arg)- and lysine (Lys)-deficient Dulbecco's modified Eagle's medium (DMEM) supplemented with 10% dialyzed fetal bovine serum (FBS), sodium pyruvate, glutamine, and gentamycin/amphoteracin and maintained in 15 cm dishes at 37 °C for at least five population doublings. Media were also supplemented with either $^{12}C_6{}^{14}N_4$-Arg and $^{12}C_6{}^{14}N_2$-Lys ("light" condition) or $^{13}C_6{}^{15}N_4$-Arg and $^{13}C_6{}^{15}N_2$-Lys ("heavy" condition). Arg was added to DMEM at one-third of the manufacturer's recommended amount. Once cells were at approximately 80% confluency, light-conditioned cells were treated with vehicle (control), and heavy-conditioned cells were exposed to 200 μM SM (experimental), a concentration that induces inflammatory cell signaling (*10, 11*) for 20 min in a certified chemical surety fume hood. For whole-cell lysate protein preparation, plates were washed 2× in ice-cold PBS and collected in lysis buffer containing 20 mM Tris-HCl (pH 7.5), 1% Triton X-100, 1 mM EDTA, 150 mM NaCl, and protease/phosphatase inhibitor tablets (Roche, Indianapolis, IN). Cells were homogenized with glass beads and a mechanical shaker for 30 s and ultracentrifuged at 20000*g* for 10 min at 4 °C. Pellets were discarded, and supernatant protein concentrations were determined by BCA assay (Pierce, Rockford, IL).

SDS-PAGE Fractionation, In-Gel Digestion, and IMAC Enrichment of Phosphopeptides. Two milligrams of total protein (1 mg of light lysate mixed with 1 mg of heavy lysate) was resolved by SDS-PAGE and briefly stained with colloidal Coomassie blue. After it was destained, the gel lane was excised into six regions, and each region was cut into 1 mm cubes. Processing for in-gel trypsin digestion was performed as described (*12*). Following trypsin digestion, IMAC (*7*) enrichment of phosphopeptides was carried out as described (*13*).

LC-MS/MS Analysis. LC-MS/MS experiments were performed on a LTQ Orbitrap hybrid mass spectrometer (Thermo Electron, San Jose, CA) as described (*14*).

Phosphopeptide Identification and Quantification. MS/MS spectra were searched via the SEQUEST algorithm (*15*) against a composite database containing the human International Protein Index (IPI) protein database and its reversed complement (*16*). Parameters allowed for up to three missed cleavages, a mass tolerance of ±100 ppm, and a static modification of 57.0215 Da for alkylation on cysteine. Dynamic modifications included 79.9663 Da for phosphorylation on serine, threonine, and tyrosine; 15.9949 Da for oxidation on methionine; and 10.0083 and 8.0142 Da on Arg and Lys, respectively, to account for the use of isotopically encoded amino acids. Search results were filtered to include <1% matches to reverse sequences by restricting the mass tolerance window and setting thresholds for Xcorr and dCn′ (*16*). We used the Ascore algorithm for phosphorylation site localization (*17*). Unique phosphorylation sites were determined by utilizing the best Ascore for each phosphorylation site to calculate the minimum number of possible phosphorylated residues on each individual protein. Phosphorylation site quantitation was performed using Vista (*18*). In cases where the same phosphorylation site was quantified multiple times, the best example in terms of Vista confidence score and minimum S/N was used (*14*). This qualitative and quantitative workflow, including SILAC labeling, IMAC enrichment, MS analysis, and peptide identification/quantitation, was carried out in triplicate ($n = 3$ biological replicates).

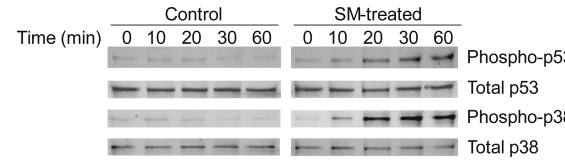

Figure 1. Confirmation of p53 and p38 phosphorylation following SM exposure. Western blot analysis of HaCaT cells that were unexposed (control, left panel) or exposed (SM-treated, right panel) to SM for 0, 10, 20, 30, and 60 min. Results showed low levels of phosphorylation for both p53 and p38 in the control samples but a steady increase in phosphorylated p53 and relatively intense p38 phosphorylation by 20 min postexposure. Total levels of p53 and p38 remained unchanged throughout the experiment. Note that contrast was increased for both the control and the SM-treated phospho-p38 panels to visualize low levels of phosphorylated protein.

Western Blotting. HaCaT cells were cultured as described above. A time−course study was conducted with cells either untreated or SM-exposed (200 μM) for 0, 10, 20, 30, and 60 min. Lysates were collected as described above. Protein (40 μg) from each time point was resolved by SDS-PAGE and transferred to nitrocellulose membrane using the iBlot system (Invitrogen, Carlsbad, CA). Western blotting was carried out using standard washing/incubation steps. Antibodies (Cell Signaling Technology, Danvers, MA) to the following proteins were used, p38 MAPK (#9212), phospho-p38 MAPK (#9211), p53 (#9282), and phospho-p53 (#9284).

Results

A time−course study was performed in HaCaT cells exposed to SM to confirm activation of p53 and p38, signaling proteins previously shown to be activated in response to SM (*10, 11*). Western blot results showed increased phosphorylation of p53 and p38 at 20 min (Figure 1), suggesting that these proteins are activated early after exposure to SM in HaCaT cells.

SILAC has proven to be an effective technique for identifying and quantifying hundreds of proteins in a single experiment and is particularly suited for signaling studies in cell culture (*5*). However, its feasibility has not been demonstrated in keratinocyte models nor in studies involving chemical warfare agents. Using SILAC, full incorporation of $^{13}C^{15}N$-labeled amino acids in HaCaT cells was accomplished after 4−5 population doublings (Supporting Information, Figure 1), a standard time frame for SILAC studies. Titration of heavy-labeled Arg was performed to determine the optimal concentration for minimizing light Arg and heavy proline (Pro) production. We selected one-third the manufacturer's recommended concentration since it resulted in the lowest production levels of both light Arg and heavy Pro (Supporting Information, Figure 1), as seen in our earlier SILAC studies (*3*). Furthermore, similar growth rates and no noticeable differences in cellular morphology were observed after three passages in culture under dialyzed FBS growth conditions (Supporting Information, Figure 2), suggesting that SILAC is a suitable technique for use in HaCaT cells.

Thus, a large-scale, quantitative analysis of the proteome using SILAC was pursued to elucidate additional cellular

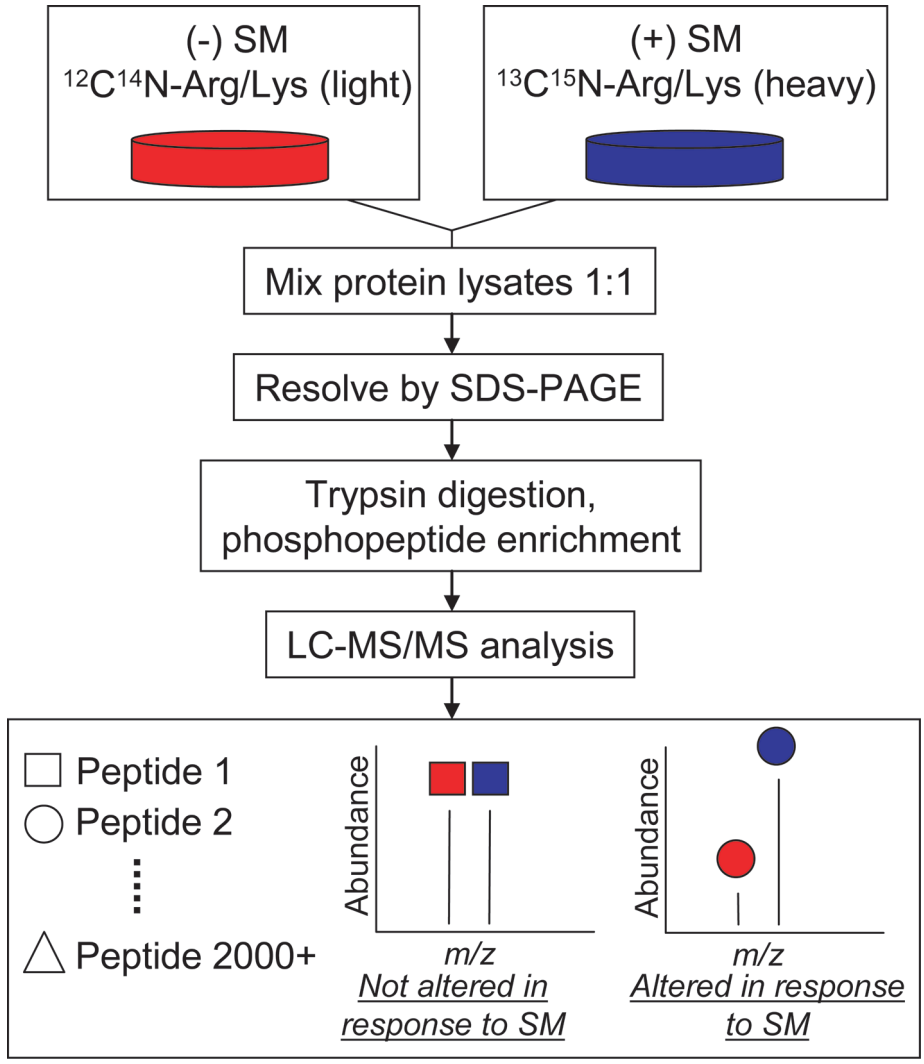

Figure 2. Flowchart of strategy used for large-scale phosphoproteomic analysis of SM-exposed cells. HaCaT cells were cultured in the presence of either isotopically "light" (control, red) or "heavy" (SM-exposed, blue) Arg/Lys. After a 20 min exposure, lysates were collected, mixed at a 1:1 ratio by protein concentration, and resolved by one-dimensional SDS-PAGE. Gel fractions were excised and in-gel-digested with trypsin. After IMAC-based phosphopeptide enrichment, samples were analyzed by high-resolution LC-MS/MS. Quantitative information was obtained by comparing the intensities of peptides originating from the heavy and light samples.

pathways and interactions activated in response to SM. The IMAC method was also employed due to the importance of protein phosphorylation in many signaling cascades (*6*). A schematic of this approach is shown in Figure 2.

This method yielded 9525 total phosphorylation sites on 4760 phosphopeptides (Supporting Information, Table 1) with a false discovery rate of less than 1%. A high degree of correlation between the experimental data set and a predicted normal distribution of quantitative ratios was also observed (Supporting Information, Figure 3), and statistical analysis resulted in a mean $\log_2$-transformed ratio of −0.089 and a $\log_2$-transformed SD of 0.55. This SD corresponded to a quantitative ratio of 1.46, indicating that phosphopeptide ratios in our data set deviating by at least 2-fold fall outside two SDs from the mean.

After excluding redundant peptides from the raw data set (Supporting Information, Table 1), our approach resulted in the confident identification of 2315 unique phosphorylation sites (Supporting Information, Table 2) from a total of 790 proteins (Supporting Information, Table 3). Peptide data were further analyzed and summarized by phosphorylated residue type (serine, threonine, and tyrosine) as well as the distribution of peptides according to number of phosphorylation sites (Supporting Information, Figure 4).

Additional filtering criteria were applied to the list of unique phosphorylation sites to compile a set of proteins containing phosphopeptides altered by at least 2-fold (increased or decreased following SM exposure). In addition to a 2-fold or greater quantitative change, these criteria required that the phosphopeptides have a signal-to-noise ratio ≥5 in the MS spectrum (for both heavy and light peptides) and a confidence score ≥85 as determined by the Vista algorithm (*18*). Phosphopeptides meeting these stringent criteria were combined and sorted into proteins, resulting in a list of 86 proteins (Supporting Information, Table 4).

The proteins in Table 1 of the Supporting Information were further analyzed by Ingenuity Pathway Analysis (IPA, Ingenuity Systems, Foster City, CA). A gene network was constructed de novo from this list based on known molecular interactions from the published scientific literature, and nearly one-third of these proteins (27/86) was found to associate through known interactions (Figure 3).

Discussion

The sequencing of the human genome and the development of gene microarray techniques have helped fuel a surge in

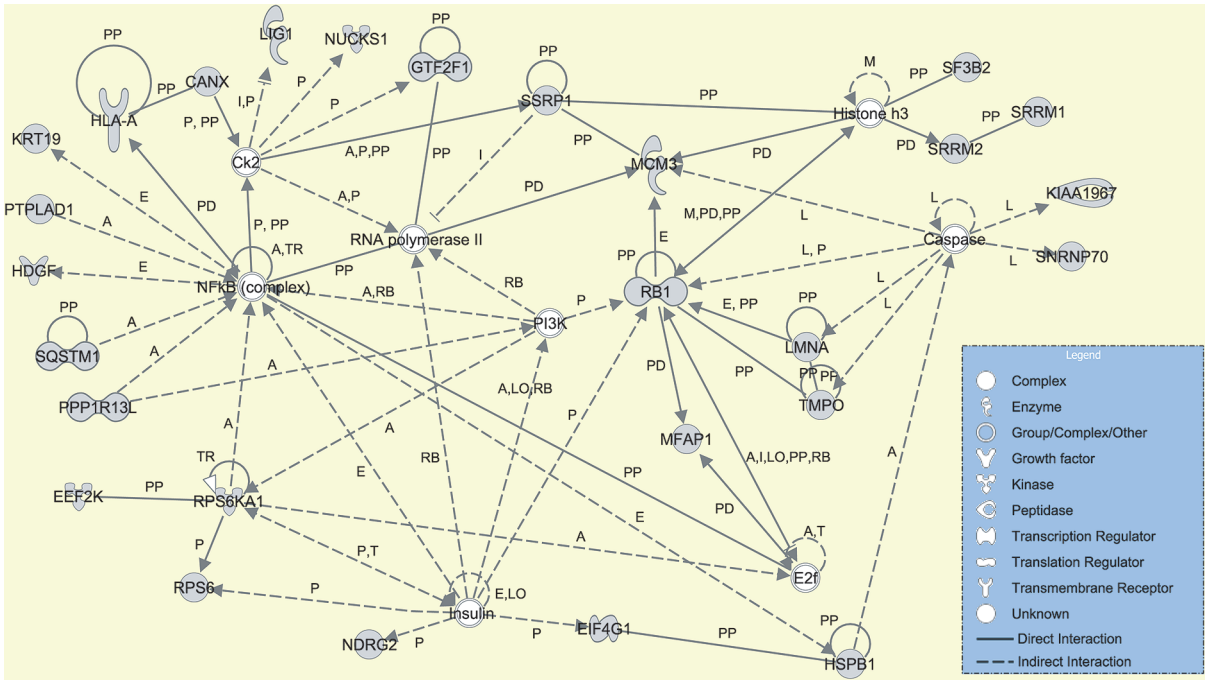

Figure 3. De novo interaction network analysis of proteins exhibiting altered phosphorylation levels in response to SM. Phosphoproteins from Table 4 of the Supporting Information were analyzed using IPA software to construct de novo interaction pathways as determined from published literature. Phosphoproteins colored gray were altered by at least 2-fold in response to SM, whereas proteins colored white were not detected in our study as exhibiting any quantitative phosphorylation change. A high confidence score of 62 was determined for this interaction map by IPA. See Table 4 of the Supporting Information for IPI numbers corresponding to each protein. Interactions shown: acts on (closed arrowhead), translocates to (open arrowhead), inhibits (T-junction), inhibits and acts on (closed arrowhead and T-junction), and binding only (simple line). "Acts on" and "inhibits" edges may also include a binding event. Abbreviations used for interactions as determined by IPA: A, activation; E, expression; I, inhibition; LO, localization; M, modification; P, phosphorylation; PD, protein−DNA interaction; PP, protein−protein interaction; L, proteolysis; RB, regulation of binding; T, transcription; and TR, translocation.

biotechnology and systems biology research efforts over the past decade. Additional innovations in genomic and proteomic technologies are examples of how far biotechnology has come in recent years. Consequently, methods that allow for studying hundreds or even thousands of genes or proteins within an organism are starting to become routine.

Likewise, the field of proteomics has been rapidly accelerated by the recent development of fast and sensitive mass spectrometry instrumentation. New methods have also been developed that take advantage of stable isotopes incorporated into the proteome, allowing for quantitative comparisons between experimental samples. Consequently, mass spectrometry can now generate both qualitative and quantitative data for thousands of proteins in a single experiment (*3*).

While proteomic methods and mass spectrometry have become powerful tools for studying various biological processes, they have yet to be fully applied within the field of chemical defense. In response, we have taken a large-scale quantitative proteomic approach to studying SM-induced toxicity using stable isotope labeling, phosphopeptide enrichment, and high-resolution mass spectrometry. Here, we report a large-scale analysis of the phosphoproteome in a cellular model of SM-induced toxicity.

This approach led to the identification of several proteins already known to be implicated in SM-induced toxicity. For example, RPS6KA1 (IPI00017305), a protein influencing NF-κB signaling (*19*), was phosphorylated nearly 3-fold higher in SM-exposed cells in this study (Supporting Information, Table 1). Earlier work by our group also detected increased phosphorylation levels of this protein following SM exposure in HaCaT cells (*10*). LIG1 (IPI00219841) was previously reported to be activated via phosphorylation in response to SM-induced DNA damage (*20*). Consistent with these results, a phosphopeptide from LIG1 was detected greater than 2-fold higher in SM-treated cells. A few additional peptides were detected with reduced levels of phosphorylation as well, although the functional significance of these phosphorylation sites in SM-exposed cells remains to be determined.

While several proteins were detected that were already known to be phosphorylated upon SM exposure, perhaps more interesting is the myriad of proteins detected that have not been previously characterized following SM-induced toxicity. Among the proteins exhibiting increased phosphorylation levels in SM-treated cells were those known to be phosphorylated following DNA damage, which occurs following SM exposure (*21*). These included RFC1 (IPI00375358), SRRM2 (IPI00748920), and SVIL (IPI00018370), each with phosphorylation levels increasing 4-fold or greater. None of these proteins have been previously reported to be implicated in SM-induced toxicity.

Similarly, SM has been shown to activate DNA damage and apoptotic responses through a variety of mechanisms, including the p53- and Bcl-2-mediated pathways (*1, 22*). TP53BP1 (IPI00029778) plays a role in the DNA damage response by enhancing p53-mediated transcriptional activation (*23*), whereas BCLAF1 (IPI00006079) is a Bcl-2-associated transcription factor involved in apoptosis by regulating p53 expression following genotoxic stress (*24*). Phosphorylation of these proteins was upregulated by at least 5-fold in SM-exposed cells.

CDK2 (IPI00031681) can be inactivated when phosphorylated at Thr-14 or Tyr-15 (*25*). However, it has been reported that this Thr-14/Tyr-15 inhibitory phosphorylation plays a relatively minor role in regulating CDK2 activity during normal cell cycle but that this inhibition can also result from DNA damage, which in turn impairs cell cycle transitions (*26*). A peptide phosphorylated at both residues was upregulated greater than 3-fold in

SM-exposed cells. This suggests an inactivation event of CDK2, consistent with SM-induced DNA damage.

Rho GTPases are known to control a variety of signaling pathways (*27*). The balance of GDP release and GTP hydrolysis on Rho is determined by guanine nucleotide exchange factors (GEFs) and GTPase-activating proteins (GAPs), respectively. Interestingly, several GEFs and GAPs were identified in this study. Phosphorylated ARHGEF11 (IPI00157442) and ARHGAP21 (IPI00169307) were detected at 2-fold lower concentrations in SM-treated cells, whereas phosphorylated ARHGAP12 (IPI217418) concentrations increased by greater than 2-fold. While the roles of GEFs and GAPs in SM-induced toxicity are unclear, future experiments could identify the downstream cellular effects of these proteins following SM exposure.

Changes in peptide phosphorylation specific to SM exposure were also characterized in this study. Indeed, these sites may point to the most interesting therapeutic targets since the levels of phosphorylation are either undetected or zero in unexposed cells. Among these are DPF2 (IPI00023322), a predicted transcription factor involved in apoptosis (*28*), and ZMYND8 (IPI00418316), a protein known to be phosphorylated upon DNA damage (*29*). Likewise, the phosphorylation of these proteins has not been previously reported to be associated with SM toxicity.

An initial concern was the absence in our data set of several changes in phosphoprotein concentrations previously implicated in SM-induced toxicity, such as p38 and p53. This can be explained by various phosphopeptide sequences not being amenable to LC-MS/MS analysis, low abundance and stoichiometry of phosphopeptides, and a limited sensitivity of the enrichment methods. These limitations may be overcome in future studies via the use of alternative proteolytic enzymes and additional fractionation steps. Nevertheless, our results represent a significant advancement in technological application of proteomics to the toxicological mechanisms following SM exposure. These results also provide a number of candidates for follow-up experiments and lead the way for additional large-scale proteomics studies.

The added value of identifying changes in specific phosphopeptide concentrations resulting from SM exposure allows for the de novo construction of SM-specific protein interaction networks. Accordingly, phosphoproteins found to be altered by at least 2-fold in response to SM and meeting additional filtering criteria (Supporting Information, Table 4) were analyzed by IPA software. The resulting network map (Figure 3) shows a number of known interactions to include events such as phosphorylation, activation, inhibition, expression, and protein−protein and protein−DNA binding. Interestingly, Ck2 was not found in our analysis, while several of its phosphorylation substrates were detected. Additionally, NF-κB and various caspases are known to respond to SM (*30, 31*), and several proteins known to be phosphorylated or otherwise interact with NF-κB and caspases were detected in our study. These results highlight the utility of this method for discovering interaction partners for proteins known—as well as unknown—to be involved in SM-induced toxicity. The exact mechanisms by which many of these proteins are phosphorylated in response to SM and their role in toxicity will be the topic of future work.

In conclusion, this study is the first attempt to quantitatively characterize the phosphoproteome following SM exposure, resulting in a list of identified phosphorylation sites that can be used as a starting point for future validation. While some of these phosphoproteins could be potential targets for therapy, these data could also be further mined using bioinformatics software to expand our understanding of phospho-specific interactions in SM-exposed cells. As methods improve and technology develops, additional phosphorylation studies can be conducted to further characterize the signaling pathways altered in response to SM and other chemical warfare agents.

Acknowledgment. Support for this work was provided by In-house Laboratory Independent Research funding from the U.S. Army (P.A.E.) as well as by the Defense Threat Reduction Agency−Joint Science and Technology Office, Medical S&T Division (J.F.D.). We thank members of the Dillman laboratory for insightful discussions and technical assistance, as well as S. Beausoleil and S. Gygi (Harvard Medical School, Boston, MA) for mass spectrometry analysis and phosphopeptide characterization. The opinions or assertions contained herein are the private views of the authors and are not to be construed as official or as reflecting the views of the Department of the Army or the Department of Defense.

Supporting Information Available: MS spectra, cellular morphology, amino acid titration data, and protein sequence and identification data. This material is available free of charge via the Internet at http://pubs.acs.org.

References

(1) Ruff, A. L., and Dillman, J. F. (2007) Signaling molecules in sulfur mustard-induced cutaneous injury. *Eplasty 8*, e2.

(2) Ong, S. E., Blagoev, B., Kratchmarova, I., Kristensen, D. B., Steen, H., Pandey, A., and Mann, M. (2002) Stable isotope labeling by amino acids in cell culture, SILAC, as a simple and accurate approach to expression proteomics. *Mol. Cell. Proteomics 1*, 376–386.

(3) Everley, P. A., Bakalarski, C. E., Elias, J. E., Waghorne, C. G., Beausoleil, S. A., Gerber, S. A., Faherty, B. K., Zetter, B. R., and Gygi, S. P. (2006) Enhanced analysis of metastatic prostate cancer using stable isotopes and high mass accuracy instrumentation. *J. Proteome Res. 5*, 1224–1231.

(4) Everley, P. A., Krijgsveld, J., Zetter, B. R., and Gygi, S. P. (2004) Quantitative cancer proteomics: Stable isotope labeling with amino acids in cell culture (SILAC) as a tool for prostate cancer research. *Mol. Cell. Proteomics 3*, 729–735.

(5) Mann, M. (2006) Functional and quantitative proteomics using SILAC. *Nat. Rev. Mol. Cell Biol. 7*, 952–958.

(6) Olsen, J. V., Blagoev, B., Gnad, F., Macek, B., Kumar, C., Mortensen, P., and Mann, M. (2006) Global, in vivo, and site-specific phosphorylation dynamics in signaling networks. *Cell 127*, 635–648.

(7) Ficarro, S. B., McCleland, M. L., Stukenberg, P. T., Burke, D. J., Ross, M. M., Shabanowitz, J., Hunt, D. F., and White, F. M. (2002) Phosphoproteome analysis by mass spectrometry and its application to *Saccharomyces cerevisiae*. *Nat. Biotechnol. 20*, 301–305.

(8) Mol, M. A., van den Berg, R. M., and Benschop, H. P. (2008) Proteomic assessment of sulfur mustard-induced protein adducts and other protein modifications in human epidermal keratinocytes. *Toxicol. Appl. Pharmacol. 230*, 97–108.

(9) Boukamp, P., Petrussevska, R. T., Breitkreutz, D., Hornung, J., Markham, A., and Fusenig, N. E. (1988) Normal keratinization in a spontaneously immortalized aneuploid human keratinocyte cell line. *J. Cell Biol. 106*, 761–771.

(10) Minsavage, G. D., and Dillman, J. F., 3rd (2007) Bifunctional alkylating agent-induced p53 and nonclassical nuclear factor kappaB responses and cell death are altered by caffeic acid phenethyl ester: A potential role for antioxidant/electrophilic response-element signaling. *J. Pharmacol. Exp. Ther. 321*, 202–212.

(11) Dillman, J. F., 3rd, McGary, K. L., and Schlager, J. J. (2004) An inhibitor of p38 MAP kinase downregulates cytokine release induced by sulfur mustard exposure in human epidermal keratinocytes. *Toxicol. In Vitro 18*, 593–599.

(12) Li, X., Gerber, S. A., Rudner, A. D., Beausoleil, S. A., Haas, W., Villen, J., Elias, J. E., and Gygi, S. P. (2007) Large-scale phosphorylation analysis of alpha-factor-arrested *Saccharomyces cerevisiae*. *J. Proteome Res. 6*, 1190–1197.

(13) Villen, J., and Gygi, S. P. (2008) The SCX/IMAC enrichment approach for global phosphorylation analysis by mass spectrometry. *Nat. Protoc. 3*, 1630–1638.

(14) Dephoure, N., Zhou, C., Villen, J., Beausoleil, S. A., Bakalarski, C. E., Elledge, S. J., and Gygi, S. P. (2008) A quantitative atlas of mitotic phosphorylation. *Proc. Natl. Acad. Sci. U.S.A. 105*, 10762–10767.
(15) Eng, J. K., McCormack, A. L., and Yates, J. R., III (1994) An approach to correlate tandem mass spectral data of peptides with amino acid sequences in a protein database. *J. Am. Soc. Mass Spectrom. 5*, 976–989.
(16) Elias, J. E., and Gygi, S. P. (2007) Target-decoy search strategy for increased confidence in large-scale protein identifications by mass spectrometry. *Nat. Methods 4*, 207–214.
(17) Beausoleil, S. A., Villen, J., Gerber, S. A., Rush, J., and Gygi, S. P. (2006) A probability-based approach for high-throughput protein phosphorylation analysis and site localization. *Nat. Biotechnol. 24*, 1285–1292.
(18) Bakalarski, C. E., Elias, J. E., Villen, J., Haas, W., Gerber, S. A., Everley, P. A., and Gygi, S. P. (2008) The impact of peptide abundance and dynamic range on stable-isotope-based quantitative proteomic analyses. *J. Proteome Res. 7*, 4756–4765.
(19) Ghoda, L., Lin, X., and Greene, W. C. (1997) The 90-kDa ribosomal S6 kinase (pp90rsk) phosphorylates the N-terminal regulatory domain of IkappaBalpha and stimulates its degradation in vitro. *J. Biol. Chem. 272*, 21281–21288.
(20) Bhat, K. R., Benton, B. J., and Ray, R. (2006) DNA ligase I is an in vivo substrate of DNA-dependent protein kinase and is activated by phosphorylation in response to DNA double-strand breaks. *Biochemistry 45*, 6522–6528.
(21) Papirmeister, B., Feister, A. J., Robinson, S. I., and Ford, R. D. (1991) *Medical Defense Against Mustard Gas: Toxic Mechanisms and Pharmacological Implications*, CRC Press, Boca Raton, FL.
(22) Rosenthal, D. S., Simbulan-Rosenthal, C. M., Iyer, S., Smith, W. J., Ray, R., and Smulson, M. E. (2000) Calmodulin, poly(ADP-ribose-)polymerase and p53 are targets for modulating the effects of sulfur mustard. *J. Appl. Toxicol. 20* (Suppl. 1), S43–49.
(23) Xia, Z., Morales, J. C., Dunphy, W. G., and Carpenter, P. B. (2001) Negative cell cycle regulation and DNA damage-inducible phosphorylation of the BRCT protein 53BP1. *J. Biol. Chem. 276*, 2708–2718.
(24) Liu, H., Lu, Z. G., Miki, Y., and Yoshida, K. (2007) Protein kinase C delta induces transcription of the TP53 tumor suppressor gene by controlling death-promoting factor Btf in the apoptotic response to DNA damage. *Mol. Cell. Biol. 27*, 8480–8491.
(25) Gu, Y., Rosenblatt, J., and Morgan, D. O. (1992) Cell cycle regulation of CDK2 activity by phosphorylation of Thr160 and Tyr15. *EMBO J. 11*, 3995–4005.
(26) Chow, J. P., Siu, W. Y., Ho, H. T., Ma, K. H., Ho, C. C., and Poon, R. Y. (2003) Differential contribution of inhibitory phosphorylation of CDC2 and CDK2 for unperturbed cell cycle control and DNA integrity checkpoints. *J. Biol. Chem. 278*, 40815–40828.
(27) Etienne-Manneville, S., and Hall, A. (2002) Rho GTPases in cell biology. *Nature 420*, 629–635.
(28) Gabig, T. G., Mantel, P. L., Rosli, R., and Crean, C. D. (1994) Requiem: A novel zinc finger gene essential for apoptosis in myeloid cells. *J. Biol. Chem. 269*, 29515–29519.
(29) Matsuoka, S., Ballif, B. A., Smogorzewska, A., McDonald, E. R., 3rd, Hurov, K. E., Luo, J., Bakalarski, C. E., Zhao, Z., Solimini, N., Lerenthal, Y., Shiloh, Y., Gygi, S. P., and Elledge, S. J. (2007) ATM and ATR substrate analysis reveals extensive protein networks responsive to DNA damage. *Science 316*, 1160–1166.
(30) Atkins, K. B., Lodhi, I. J., Hurley, L. L., and Hinshaw, D. B. (2000) N-acetylcysteine and endothelial cell injury by sulfur mustard. *J. Appl. Toxicol. 20* (Suppl. 1), S125–S128.
(31) Simbulan-Rosenthal, C. M., Ray, R., Benton, B., Soeda, E., Daher, A., Anderson, D., Smith, W. J., and Rosenthal, D. S. (2006) Calmodulin mediates sulfur mustard toxicity in human keratinocytes. *Toxicology 227*, 21–35.

TX900265Z